EFFECT OF THERMAL STRESSES ALONG CRACK SURFACE ON ULTRASONIC RESPONSE

I. Virkkunen[1], M. Kemppainen[2], J. Pitkänen[3] and H. Hänninen[1]

[1]Helsinki University of Technology, FIN-02015, Espoo, Finland
[2]Trueflaw Ltd. Tekniikantie 21, P.O.Box 540, FIN-02151, Espoo, Finland
[3]VTT, Kemistintie 3, Espoo, Finland

ABSTRACT. Artificial flaws can be manufactured by controlled thermal fatigue loading. The produced cracks can be introduced to a wide variety of materials. This technology gives also a unique opportunity to monitor the ultrasonic response of a crack during thermal loading.
This paper reports studies on the effects of different thermal load cycles on the ultrasonic response. The loads are analyzed with FEM. Two cracked samples were loaded with different thermal load cycles.

INTRODUCTION

Thermal loads have been identified as the primary cause of cracking in several published failure analysis in the nuclear industry [1,2]. Typical sources of thermal loads include turbulent mixing, striping and stratification of fluids in different temperature in T-joints. Rapid temperature changes can cause repeated, high local strains. The temperature variations that arise due to fluid mixing are difficult to predict and consequently the resulting thermal loads are difficult to design for.
While the thermal loads in the actual industrial applications are often difficult to predict, in laboratory conditions thermal loads can be applied with high controllability and repeatability. Thermal loads can be used to induce high local strains to thick sections and heavy components. This is useful, e.g., for producing artificial flaws to heavy components in-situ. In present paper thermal loads are used to study the effect of loading to ultrasonic response of cracks in heavy sections.

THERMAL LOADS

Change in temperature induces thermal expansion of the material. If this expansion is hindered, thermal stresses arise. Thermal stresses can arise because of either external or internal constraints. Internal constraints can be caused by nonuniform temperature distribution or nonuniform material properties. The elementary theory of thermal stresses is quite well established, see e.g. [3]. Nevertheless, thermal loads and especially thermal fatigue remain difficult to design for due to the complex circumstances that can lead to thermal fatigue damage.
Thermal loads caused by nonuniform temperature distribution resulting , e.g., from rapid temperature changes on pipe wall have some characteristics that are noteworthy for present

discussion. The rate of temperature change is highest on the surface, where the thermal flux is controlled by the heat transfer coefficient between the pipe wall and the fluid inside. Rate of temperature change deeper within the material is limited by the thermal conductivity of the material and thus both the rate of temperature change and temperature range decrease with increasing depth. Consequently, also the thermal stresses are highest at the surface. The stresses are self-equilibrating, i.e. compressive stress at the surface must be balanced by tensile stress deeper in the material and vice versa.

MATERIALS AND METHODS

Experiments were performed with special thermal fatigue test equipment [4] utilizing high frequency induction heating and water or air spray cooling. Tests were performed with two different specimens both of which are representative nuclear components: a primary pipe sample (A) and a BWR core spray nozzle safe end (B). A thermal fatigue crack was produced to both specimens. Crack behaviour under thermal fatigue loading was monitored in both specimens ultrasonically and additionally by a digital video camera in specimen A. The videotape was used to analyze the crack opening behaviour during each cycle.

Samples

Sample A was a centrifugally cast large grain austenitic stainless steel sample representing a primary pipe with 845 mm outer diameter, appr. 190 mm circumferential by 400 mm axial and 60 mm thick [5]. The material grade was ASTM A-351 Grade CF-8A (cast 304). The sample contained a 34 by 17 mm thermal fatigue crack, which was thermally loaded during the experiment. The sample is shown in Figure 1.
Sample B was a core spray nozzle constructed from three different materials: A508 carbon steel, Inconel 600 and AISI 316 type austenitic stainless steel. The weld filler material used for both of the welds was Inconel 182 with Inconel 82 root pass. The sample contained a 14.2 by 5 mm thermal fatigue crack in Inconel 600 heat affected zone, which was loaded thermally during the experiment. The sample is shown in Figure 1.

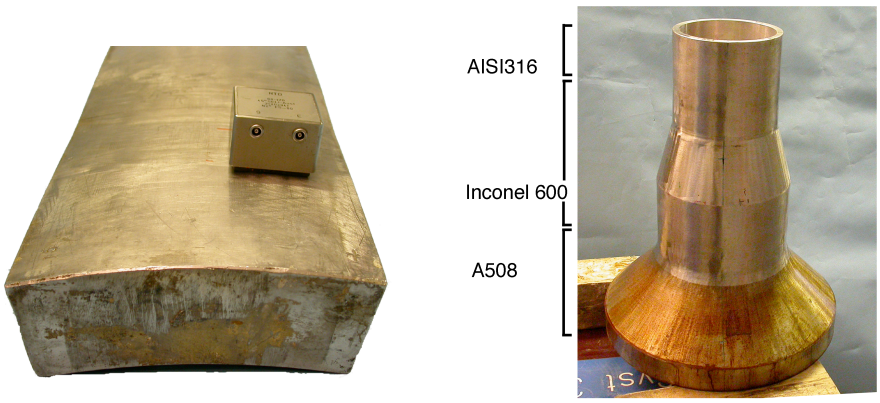

FIGURE 1. Used samples. Sample A, a cast austenitic stainless steel pipe section is shown on the left. Sample B, a core spray nozzle is shown on the right. In sample A the crack is located in the heat affected zone (HAZ) parallel to weld. In sample B the crack was located in Inconel 600 HAZ parallel to the weld.

Applied loads

The cracked samples were loaded by successive heating by high frequency induction and water spray cooling. The applied thermal cycles are presented in Figure 2. For sample

A single thermal cycle was analyzed (marked A1), whereas for sample B two different cycles were chosen for analysis (marked B1 and B2).

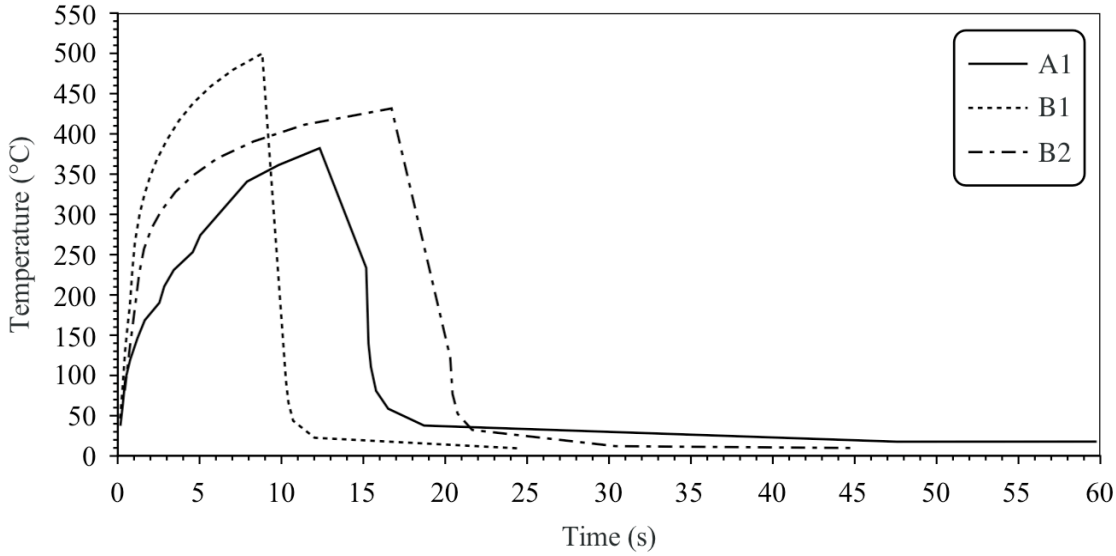

FIGURE 2. Temperature curves from load cycles. Sample A was loaded with one temperature cycle (A1) with temperature ranging from 20 to 350 °C. Sample B was loaded with two different temperature cycles: a faster cycle with ΔT= 20 ... 500 °C (B1) and a slower cycle with ΔT = 20 ... 430 °C (B2).

NDT set up

The NDT set-up used in the study is described in more detail in related papers [6,7]. In sample A the crack was monitored with 1 MHz 45° TRL-probe. In sample B the crack was monitored with 1.5 MHz 41° transverse wave probe.

FEM analysis

The loads were analyzed by one-dimensional linear-elastic model (Figure 3). The model was loaded with temperatures measured on the sample surface (Figure 2). The numerical cycle was allowed to stabilize for nine cycles and the strains were solved for the tenth thermal cycle. Calculation was performed with ANSYS FE-code.

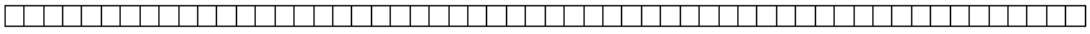

FIGURE 3. The FEM mesh used.

RESULTS AND DISCUSSION

Analysis of applied loads

The resolved temperature distributions are presented in Figures 4 – 6. The temperature variation during a cycle is greatest at the sample surface and diminishes with increasing depth. It should be noted, that the moment of highest temperature is different at different depths, especially for the faster cycles. E.g. for cycle B1 the highest temperature at depth of 10 mm is reached during the cooling phase, while the surface temperature is already decreased near to its minimum.

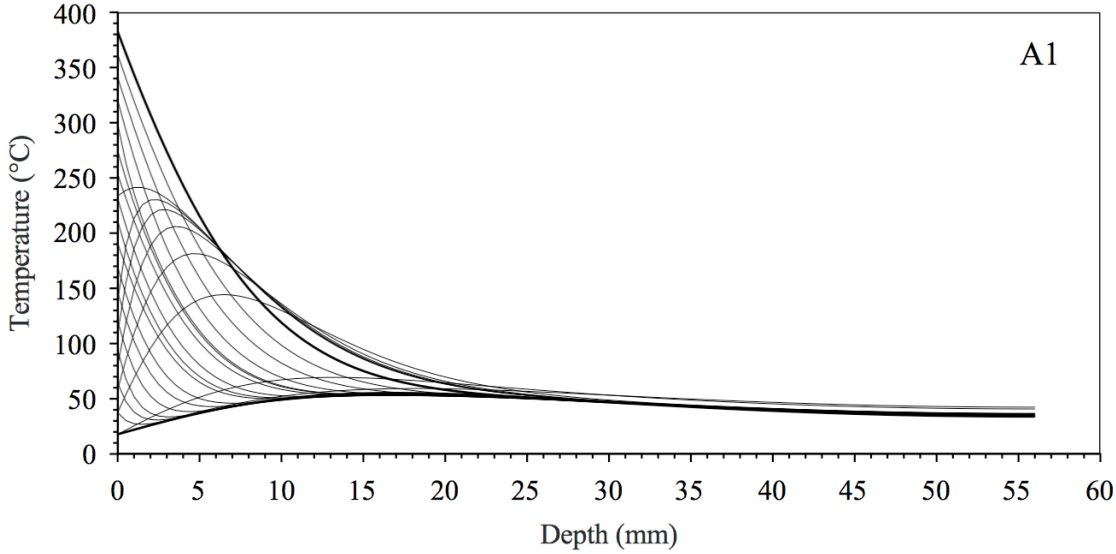

FIGURE 4. Temperature distributions calculated for thermal cycle A1 for sample A.

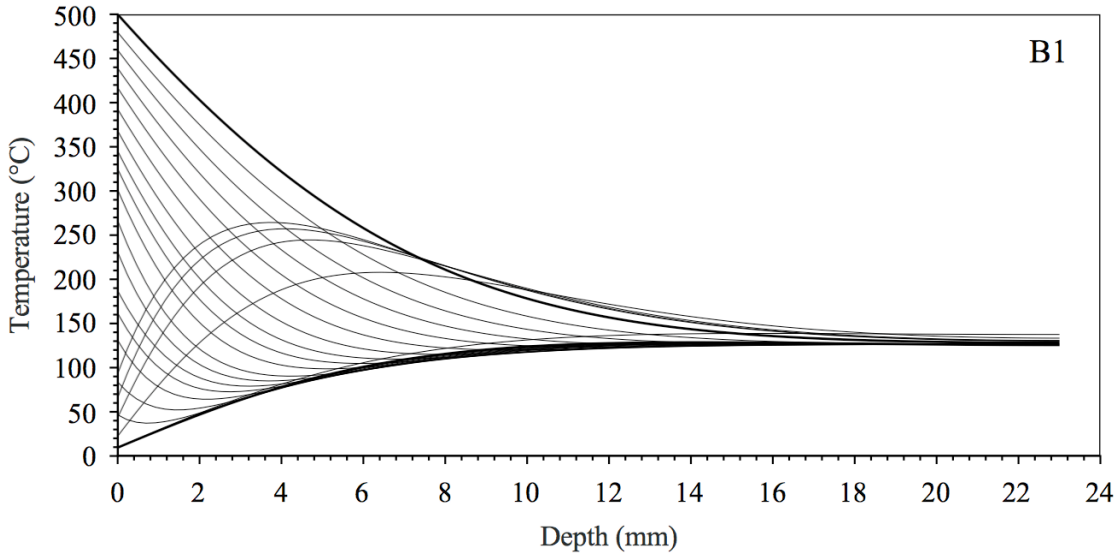

FIGURE 5. Temperature distributions calculated for thermal cycle B1 for sample B.

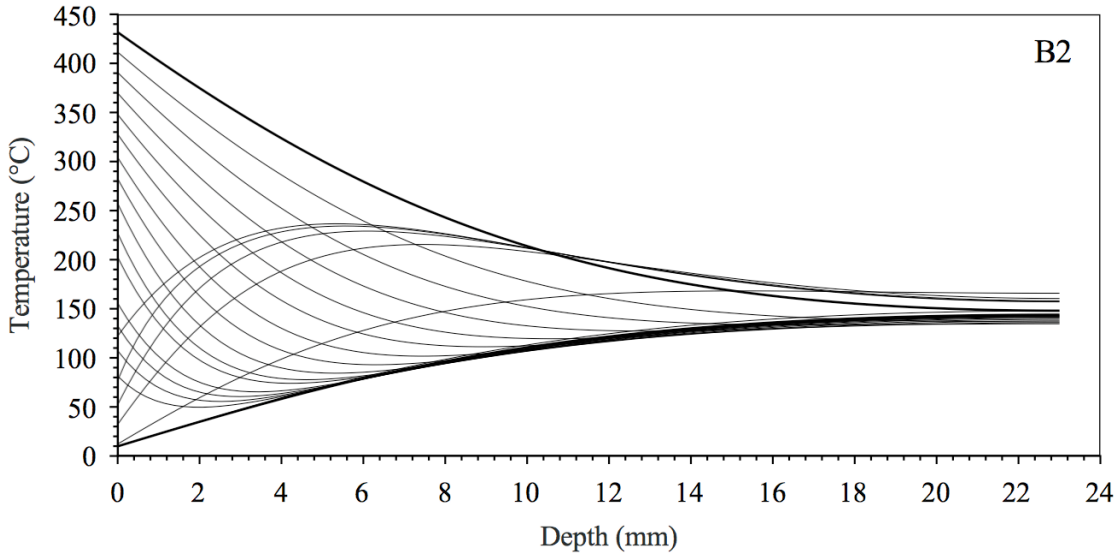

FIGURE 6. Temperature distributions calculated for thermal cycle B2 for sample B.

The resolved strain distributions are presented in Figures 7 – 9. Each strain curve, i.e. each time step, describes a self-equilibrating strain state, with compressive strains balanced by tensile strains and a point of zero strain in between. Also the strain range during a cycle is greatest at the sample surface and diminishes with increasing depth as seen from the envelope curve. However, as the point of zero stress is at different depth for each point in time, the strain range over the whole cycle does not diminish completely at any depth. Instead, the thermal loads at the surface give rise to significant strain variation at surprisingly high depths and enable through wall crack growth.

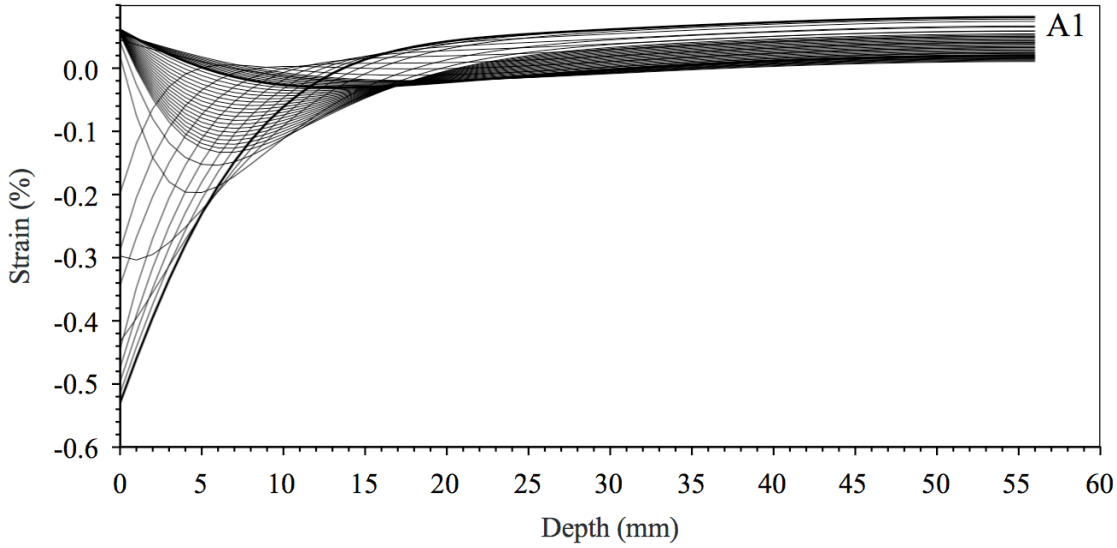

FIGURE 7. Strain distributions calculated for thermal cycle A1 and sample A.

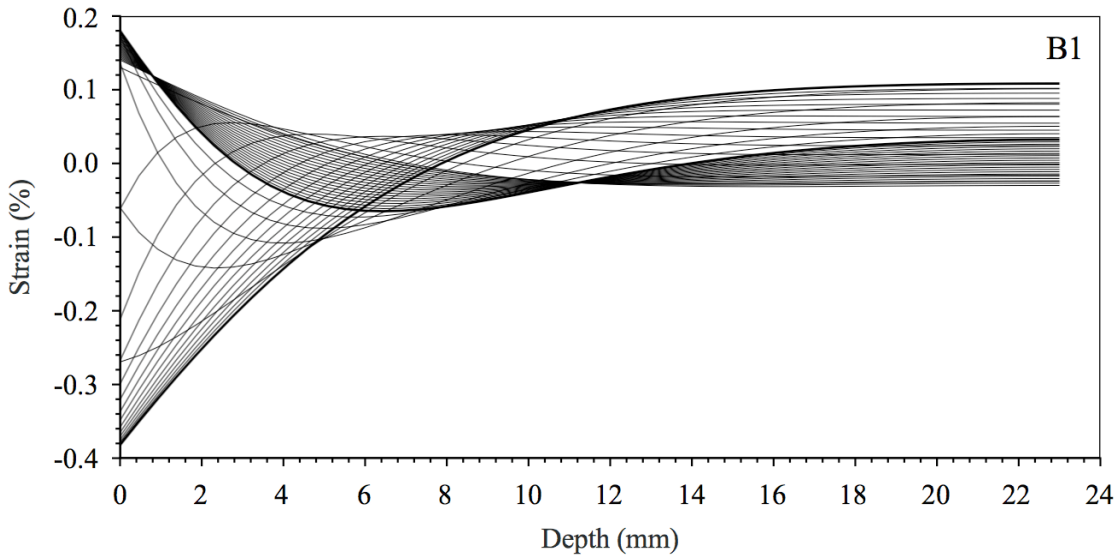

FIGURE 8. Strain distributions calculated for thermal cycle B1 and sample B.

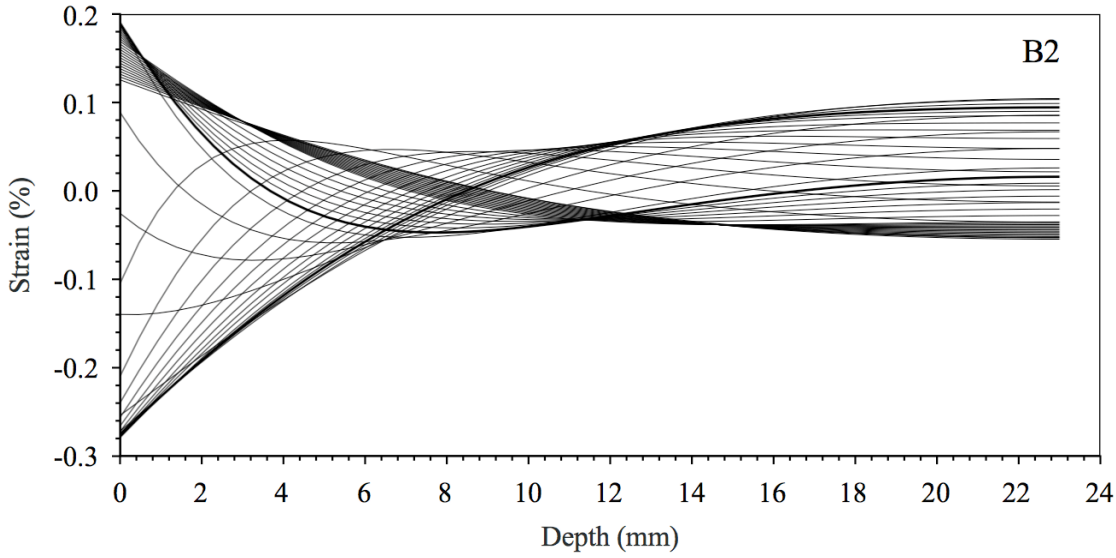

FIGURE 9. Strain distributions calculated for thermal cycle B2 and sample B.

Ultrasonic response

The ultrasonic response was monitored during loading. Figure 10 presents two typical A-scans from different parts of the thermal cycle. In Figures 11 – 13, the calculated strain over time at different depths is shown together with measured ultrasonic amplitude from corner echo and crack tip echo. It is seen, that the corner echo amplitude decreases markedly during heating, as the surface is under compressive strains in sample B. Sample A shows contradictory behaviour: corner amplitude increases with compressive loads. This behaviour can be attributed to the bigger crack size in sample A. For bigger crack (and for lower frequency probe) the corner signal comes from larger volume than for small crack. Hence the corner echo amplitude is not directly related to the surface load.

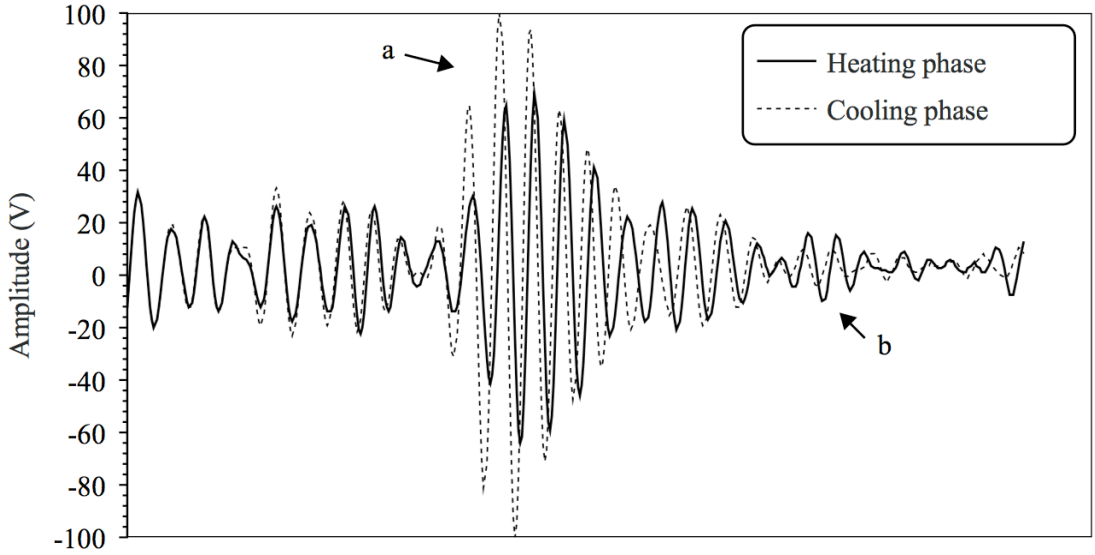

FIGURE 10. Typical A-scans of heating and cooling phase from sample B and cycle B1. In the corner echo (a) the amplitude decreases 4.0 dB during heating phase, as the crack mouth is under compressive strains whereas the crack tip echo (b) increases 4.1 dB during heating.

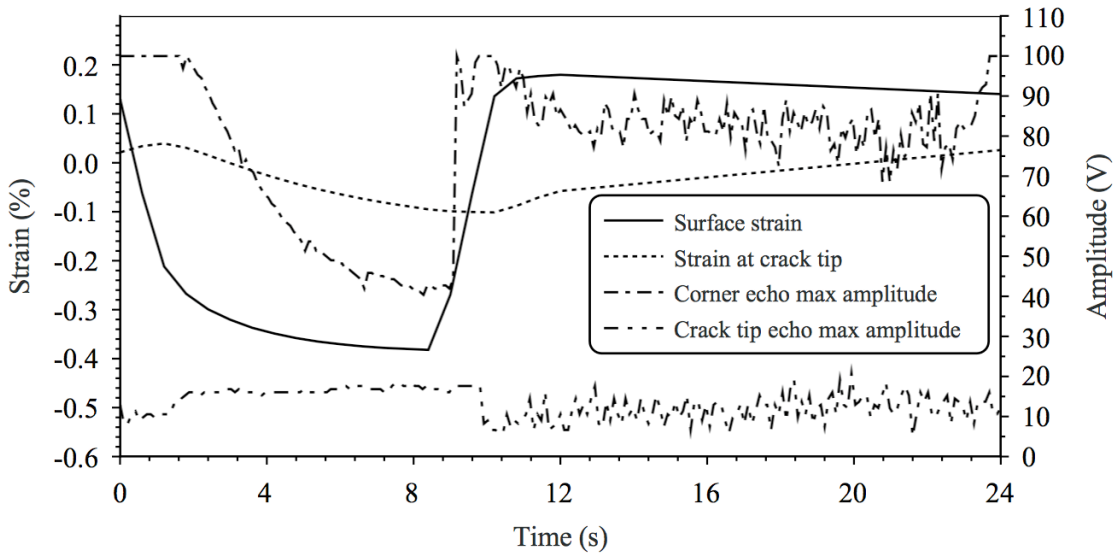

FIGURE 11. Calculated strain and measured UT amplitude curves over time for cycle B1.

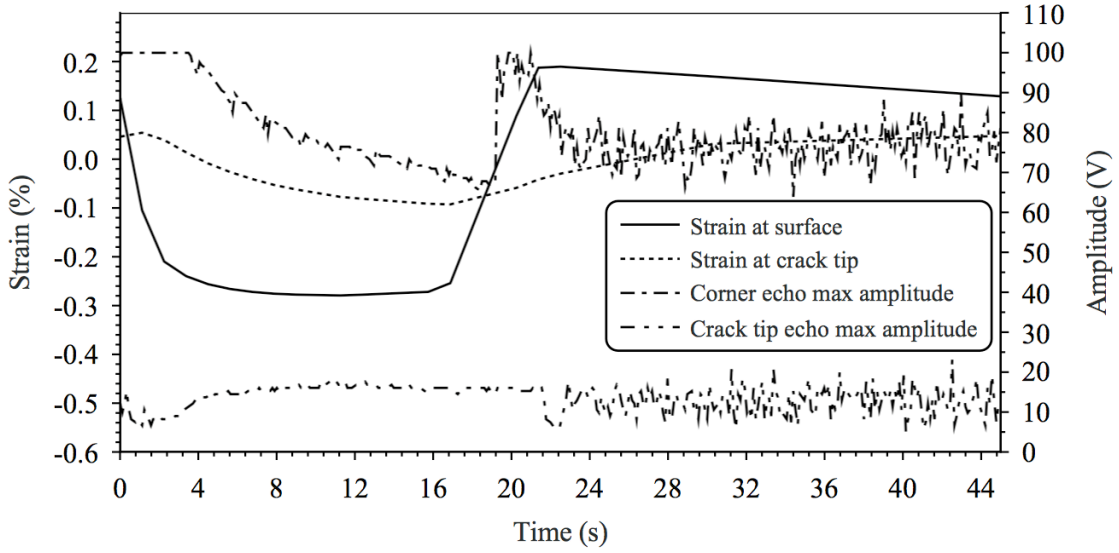

FIGURE 12. Calculated strain and measured UT amplitude curves over time for cycle B2.

Video monitoring

The crack opening was monitored by a video camera during the loading. Figure 13 shows the crack opening measured from the video image as a function of time together with UT amplitude and calculated strains. The crack closes during heating (surface under compressive strains) and opens during cooling (surface under tensile strains). However the moment of zero crack opening does not coincide with calculated moment of zero surface strain. This is due to two factors. Firstly, the opening is affected by the strains over the whole crack depth, and calculated tensile strains deeper along the crack face can cause the crack to open even under calculated compressive surface strains. Secondly, The calculated strains exceed the nominal yield strain of the material. Consequently the thermal strains have left residual stresses in the material that make the cycle more symmetric. In the surface layer this means, that the cycle is shifted towards tensile strains and hence, the crack opens earlier than expected.

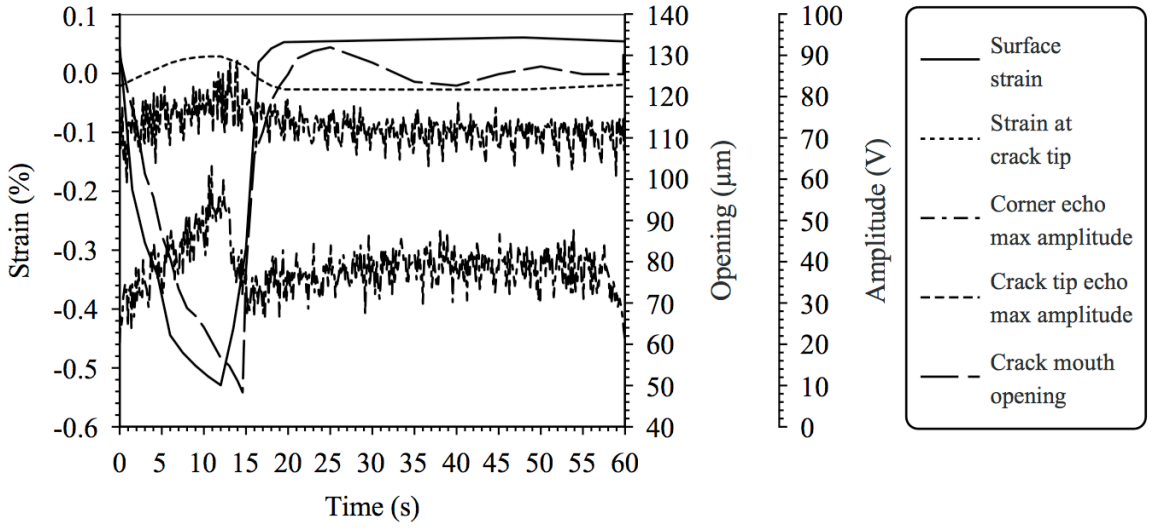

FIGURE 13. Calculated strain and measured UT amplitude curves over time for thermal cycle A1 and sample A. Crack mouth opening follows the calculated (compressive) strains with a small delay.

CONCLUSIONS

The ultrasonic response of a crack is significantly altered by loading. These alterations can be explained by their effect on the crack opening. However, with complex loads, e.g. thermal loads, the ultrasonic response is affected by the loads over the whole crack length and compressive loads near the surface can either increase or decrease the measured amplitude, depending on the crack depth and load cycle.

REFERENCES

1. Hänninen, H. and Hakala, *J. International Journal of Pressure Vessels & Piping* **9**, 445-455 (1981).
2. Cipiere, M. F. and Le Duff, J.A., "Thermal fatigue experience in French piping : influence of surface condition and weld local geometry," in Proceedings of IIW meeting of the commission XIII on fatigue, International Institute Of Welding, IIW – XIII-1891-01, 2001.
3. Boley, B. A. and Weiner, J. H., *Theory of Thermal Stresses*, John Wiley & Sons, Inc., New York, 1960, 586 p.
4. Kemppainen, M., *Design and Implementation of Thermal Fatigue Testing Facility*, Master's Thesis, Helsinki University of Technology, Laboratory of Engineering Materials, Report MTR 1/97, Espoo, 1997, 121 p.
5. Bates, S. R., Doctor, S. R. and Heasler, P.G, *Stainless Steel Round Robin Test Centrifugally Cast Stainless Steel Screening Phase*, NUREG/CR-4970, PNL-6266, PISC III Report No. 3, Pacific Northwest Laboratory, 1987.
5. Pitkänen, J., Kemppainen, M. and Virkkunen, I. "Ultrasonic Study Of Crack Under A Dynamic Thermal Load," in *QNDE Conference Proceedings*, to be published.
6. Kemppainen, M., Virkkunen, I., Pitkänen, J. and Hänninen, H., "Advanced Flaw Manufacturing and Crack Growth Control," ibid.